Supporting Information for "Geodetic matched filter slow slip event detection along the northern Japan subduction zones"

Lou Marill[1], David Marsan[1], Baptiste Rousset[2]and Anne Socquet[1]

[1]Univ. Grenoble Alpes, Univ. Savoie Mont Blanc, CNRS, IRD, Univ. Gustave Eiffel, ISTerre, 38000 Grenoble, France

[2]Institut Terre et Environnement de Strasbourg, Université de Strasbourg, CNRS, 67000 Strasbourg, France

Contents of this file

Detection ID	Time (year)	Longitude	Latitude	Duration (days)	M_w
01	2000.630	140.77	35.57	14	6.1
02a	2002.766	140.57	34.99	14	6.5
02b	2002.842	140.42	34.95	24	5.9
03	2005.034	141.11	35.44	08	6.1
04	2005.297	139.69	36.21	42	5.8
05	2006.111	140.31	35.13	14	5.7
06	2007.621	140.63	35.00	18	6.5
07	2009.086	141.15	35.23	38	6.4
08	2009.968	140.70	34.93	08	6.2
09	2010.215	141.18	35.16	26	6.2
10	2011.829	140.52	34.96	18	6.6
11	2014.010	140.70	34.97	18	6.5
12	2018.442	140.57	34.98	18	6.7

Table S1. Parameters estimated for the detections on the PHS plate. Longitude and Latitude correspond to the coordinates of the barycenter of the detections.

Detection ID	Time (year)	Longitude	Latitude	Duration (days)	M_w
01	2000.939	141.11	34.73	06	6.3
02	2003.738	141.96	40.23	38	6.5
03	2004.807	142.51	39.30	06	6.6
04	2010.785	142.10	39.03	26	6.3
05	2012.037	141.95	40.25	08	6.5
06	2012.094	143.33	41.02	10	6.7
07	2014.533	140.72	34.54	10	6.4
08	2016.908	143.02	40.10	24	6.5
09	2018.081	141.57	40.58	08	6.3

Table S2. Parameters estimated for the detections on the PAC plate. Longitude and Latitude correspond to the coordinates of the barycenter of the detections.

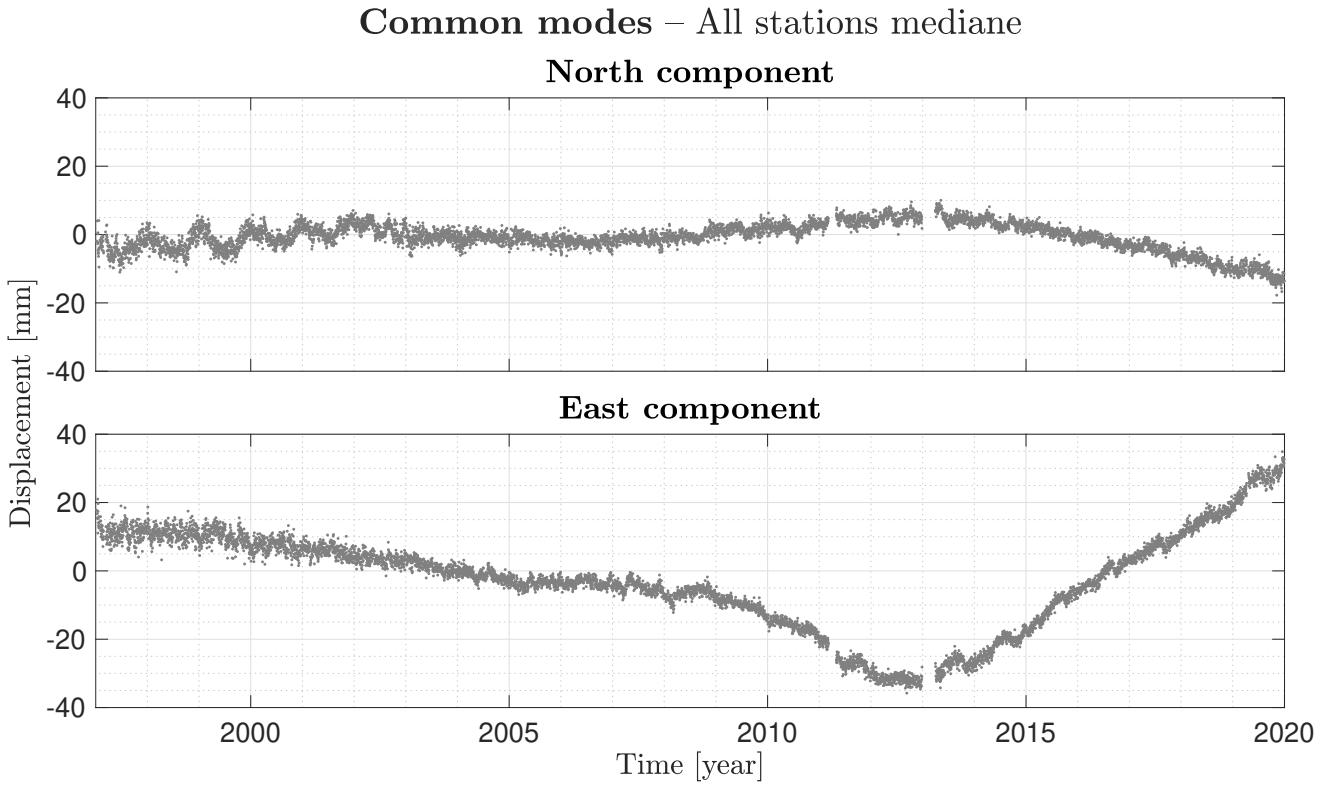

Figure S1. Common modes removed from the GNSS time series that correspond to the median over the network. The top panel corresponds to the north component and the bottom panel to the east component.

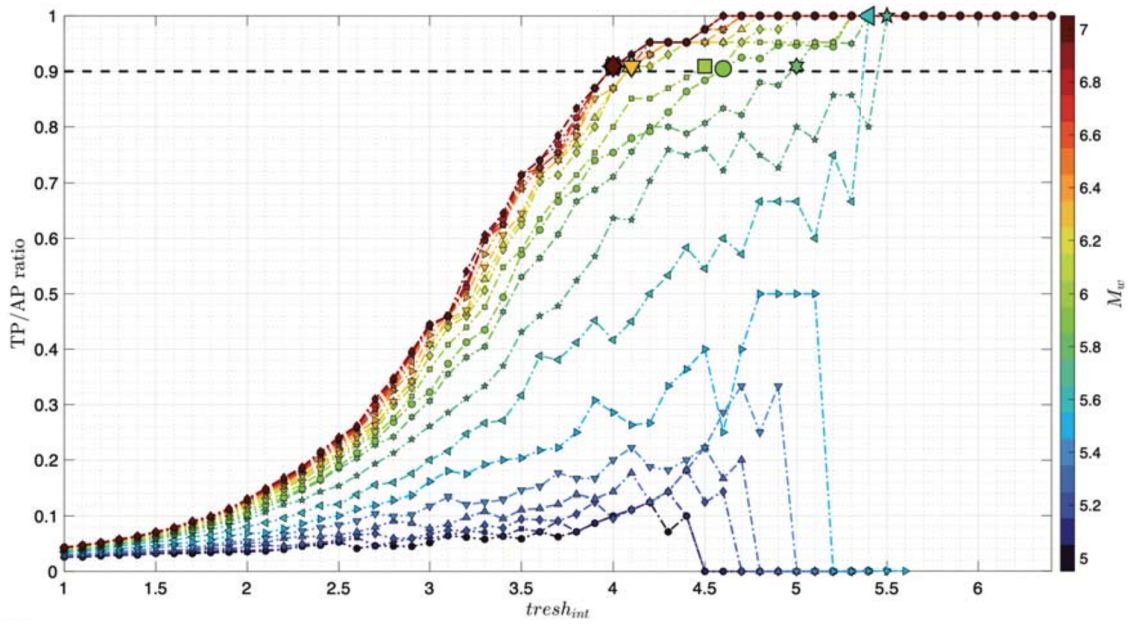

Figure S2. True Positive detections / All Positive (TP/AP) ratio as a function of the detection threshold $tresh_{int}$ for the patch 245 of the Philippine Sea plate represented in Figure 3. The curves represent the median results for 10 synthetic data sets with synthetic transient slip events of M_w from 5.0 to 6.5. Each color corresponds to the TP/AP ratio curve for the M_w shown in the colorbar. The black dotted line represents the 90% TP/AP ratio, and the symbol the associated detection treshold.

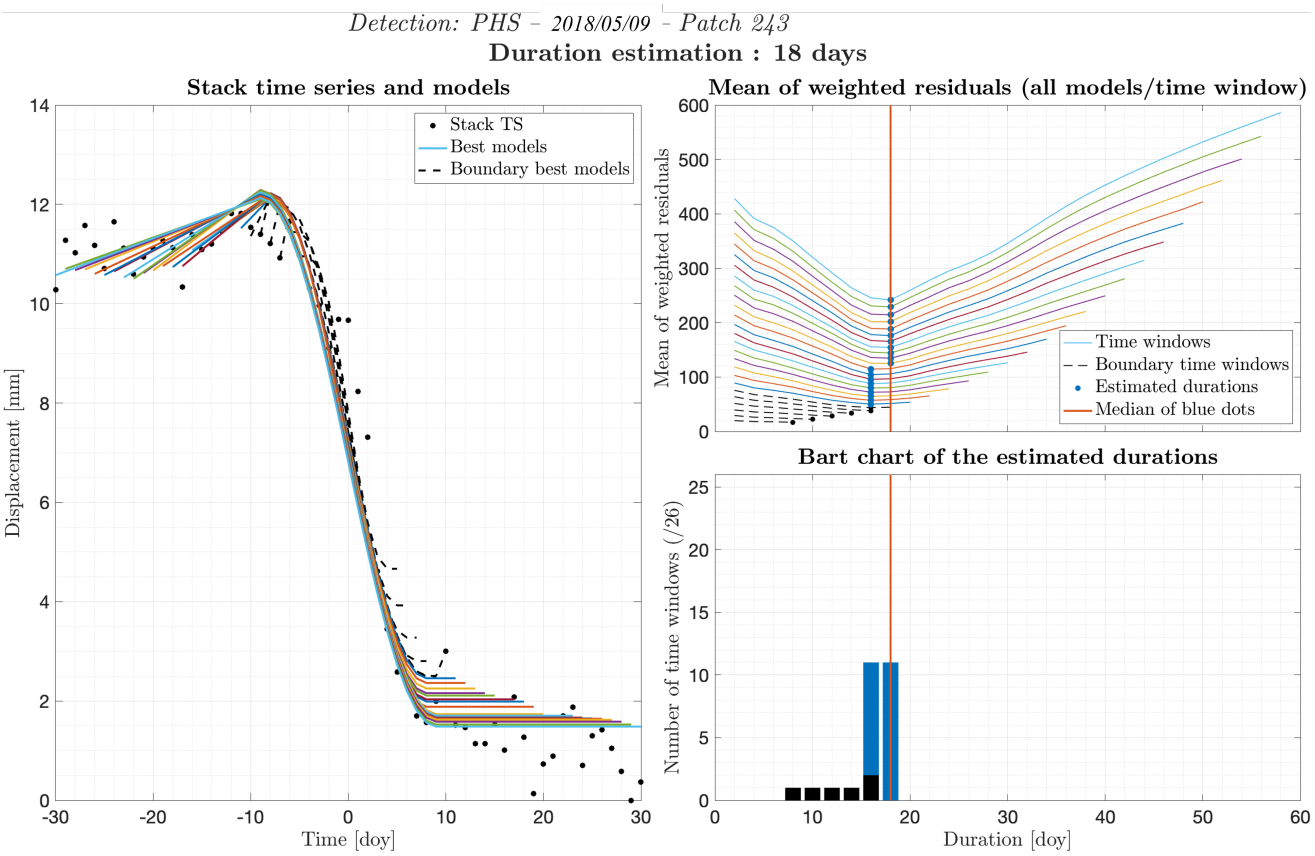

Figure S3. Example of estimation of the duration for the event detected on 2018/05/09. (Left) The GNSS stacked time series centered on the detection time is represented with the black dots. The model for the best Δ of each window D is shown by the colored lines. The dashed lines represents the models for which the best Δ hits the edge of the considered time window D. (Top right) RMSE as a function of the duration of the time windows tested. The best Δ values that minimize the residuals are highlighted by the blue dots. The red line outlines the final (best) estimation. (Bottom right) Histogram of the best Δ values for all the tested time windows.

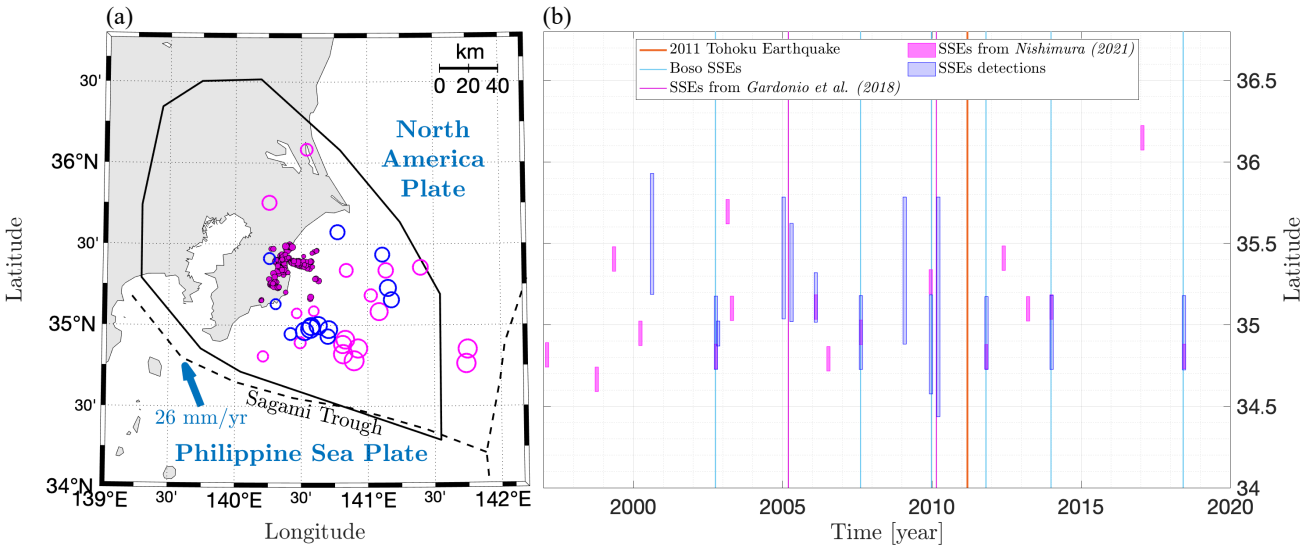

Figure S4. Comparison between the detected SSEs in this study on the Philipine Sea plate and Nishimura (2021)'s probable SSEs detections. Same legend as Figure 6, except that the open circles in (a) and open bars in (b) corresponds to the detection of the two catalogs: blue for our study and magenta for Nishimura (2021).

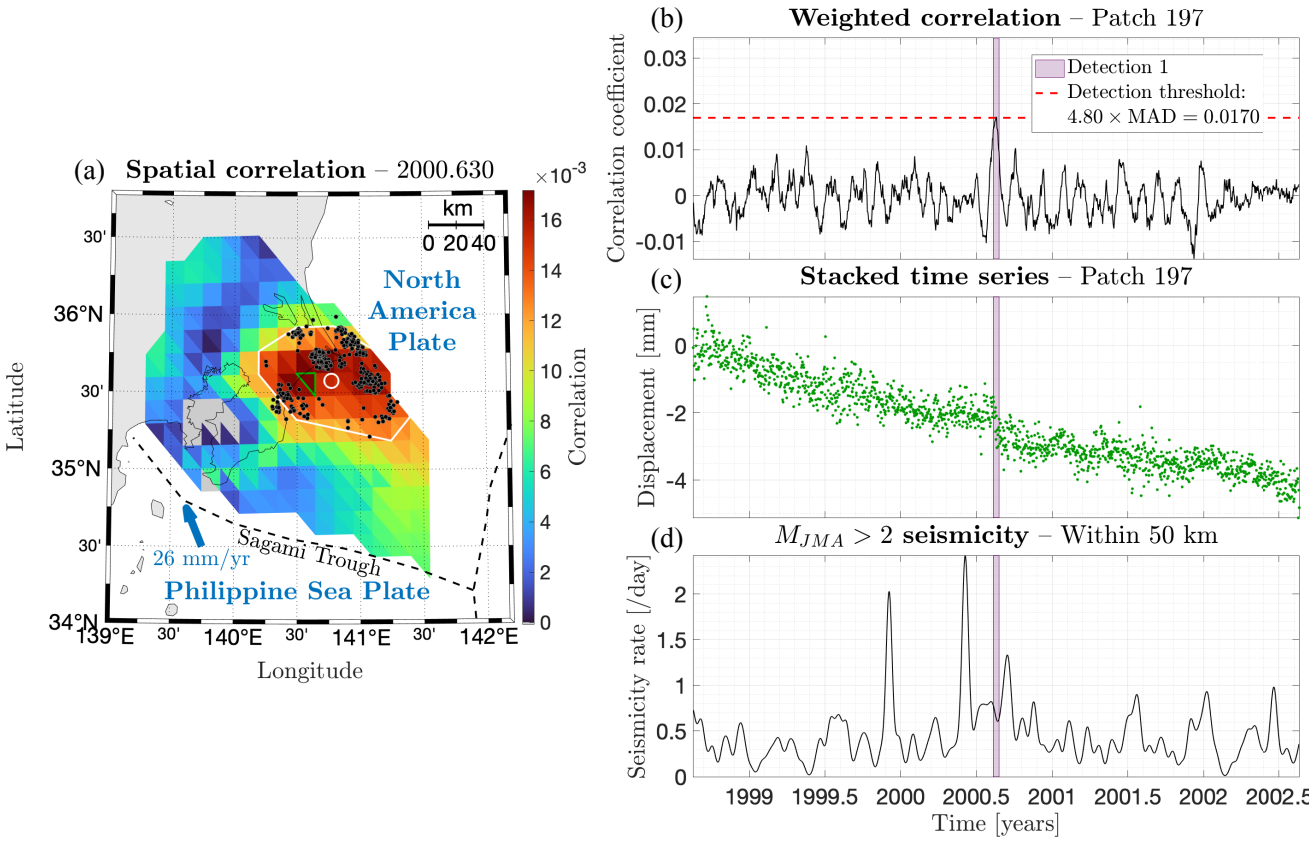

Figure S5. Detection of event 1 of the PHS plate. (a) Amplitude of the correlation on the plate interface. The green triangle highlights the patch with the largest correlation amplitude. The white line indicates the 75% contour, with the white circle corresponding to its barycenter. (b) Time series of the correlation function. The dashed red line indicates the detection threshold. The purple rectangle shows the detected event. Blue rectangles show the location of the known Boso SSEs. (c) GNSS weighted stacked time series. (d) Daily seismicity rate averaged over a 7-day time window from the $M_{JMA} > 2$ events within a radius of 50 km from the white circle. Grey stars indicate the $M_{JMA} > 6.4$ events within a radius of 200 km from the white circle.

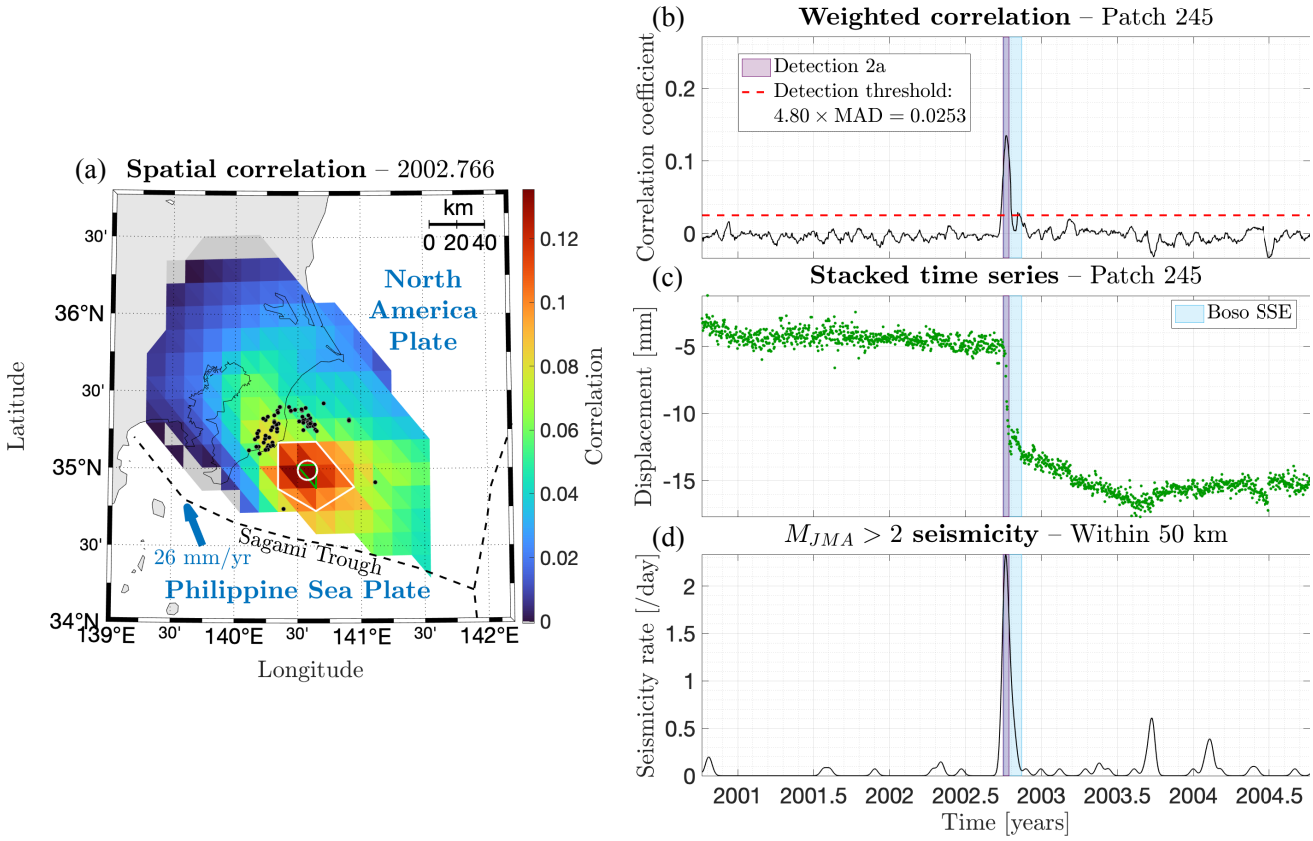

Figure S6. Same as Figure S4, but for event 2a detected on the PHS plate.

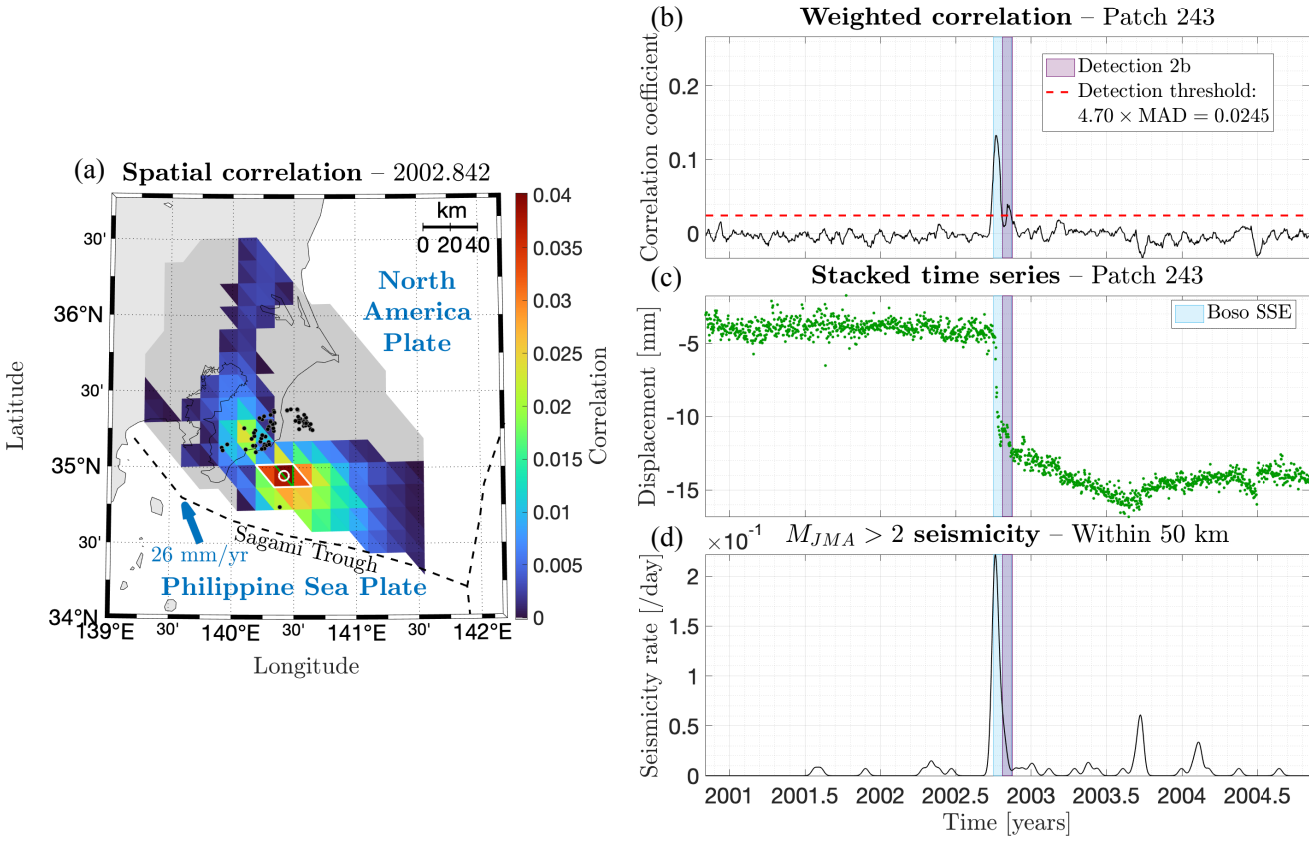

Figure S7. Same as Figure S4, but for event 2b detected on the PHS plate.

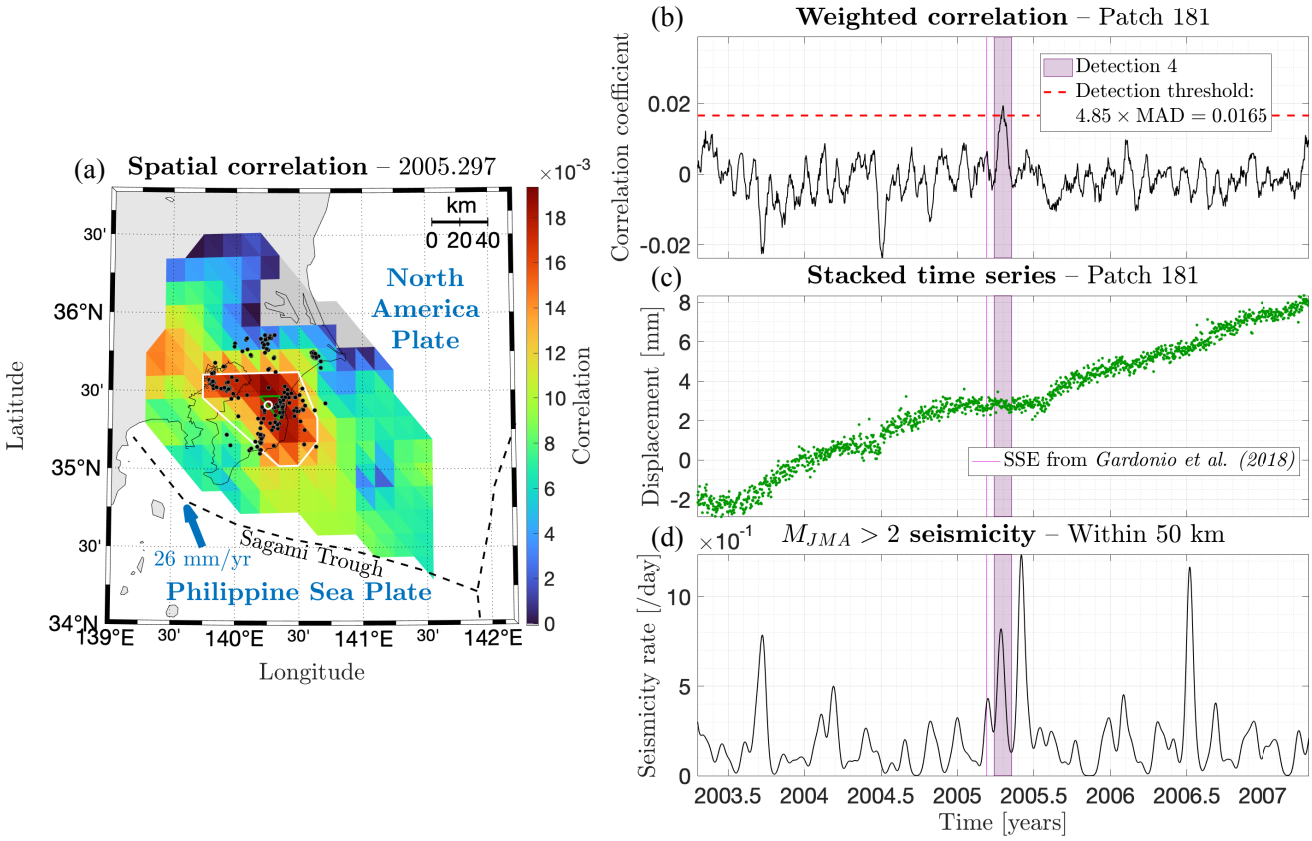

Figure S8. Same as Figure S4, but for event 4 detected on the PHS plate.

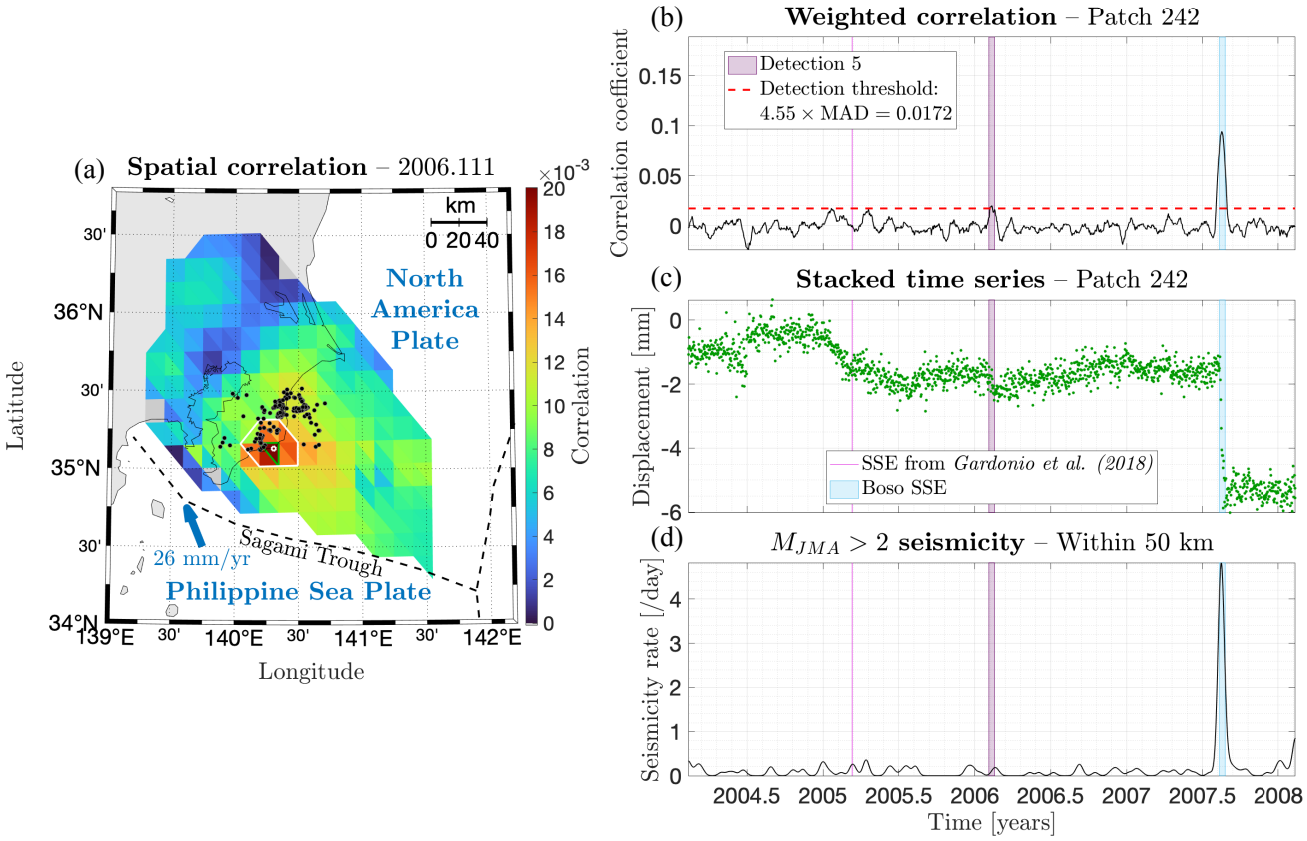

Figure S9. Same as Figure S4, but for event 5 detected on the PHS plate.

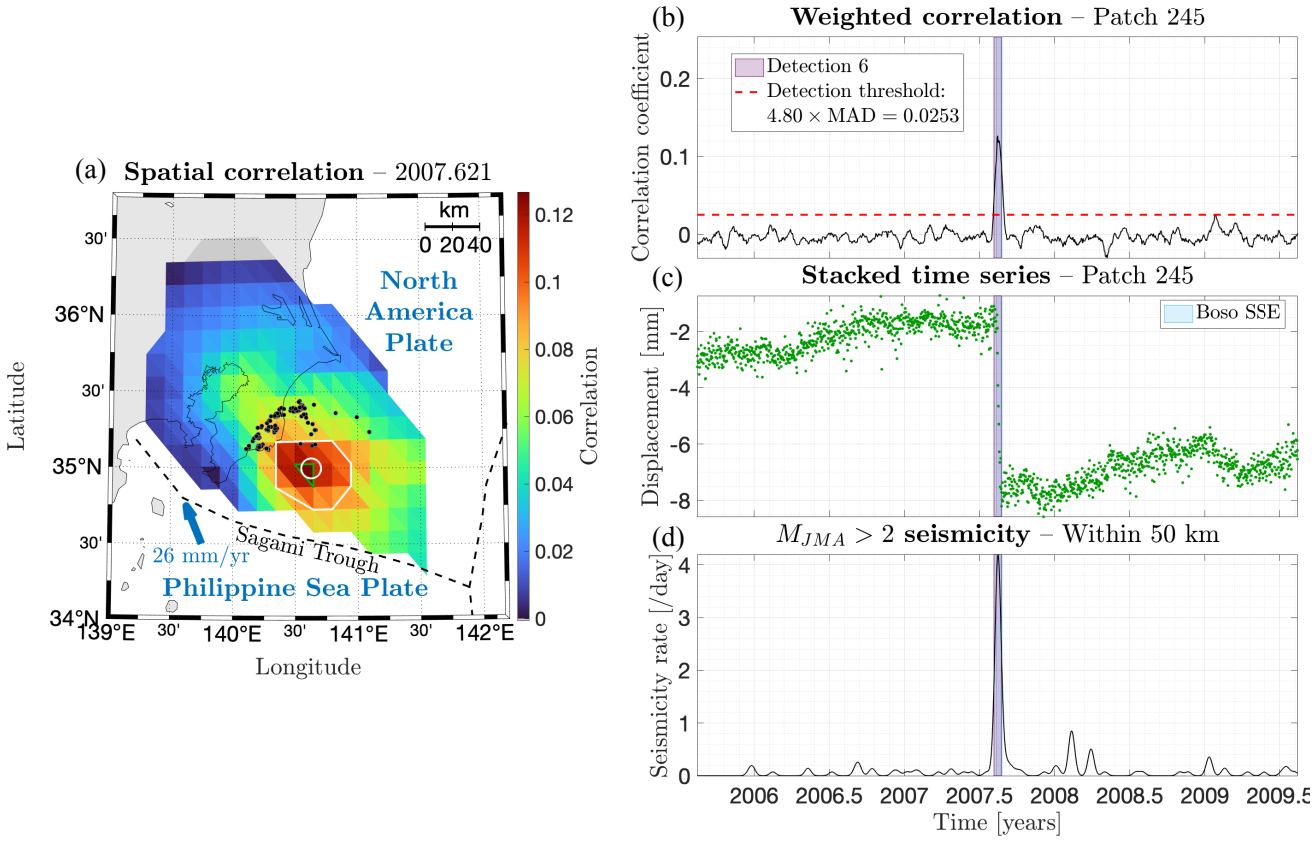

Figure S10. Same as Figure S4, but for event 6 detected on the PHS plate.

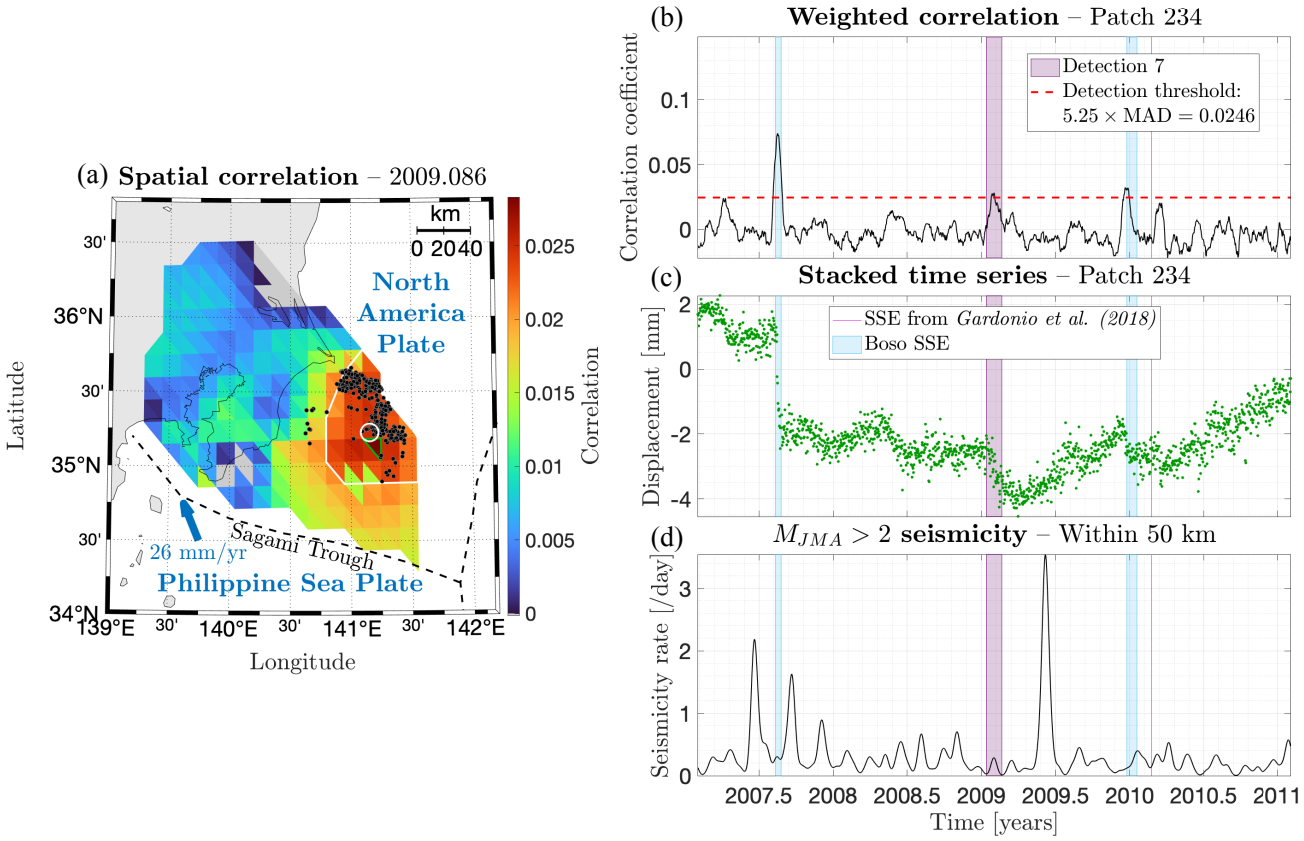

Figure S11. Same as Figure S4, but for event 7 detected on the PHS plate.

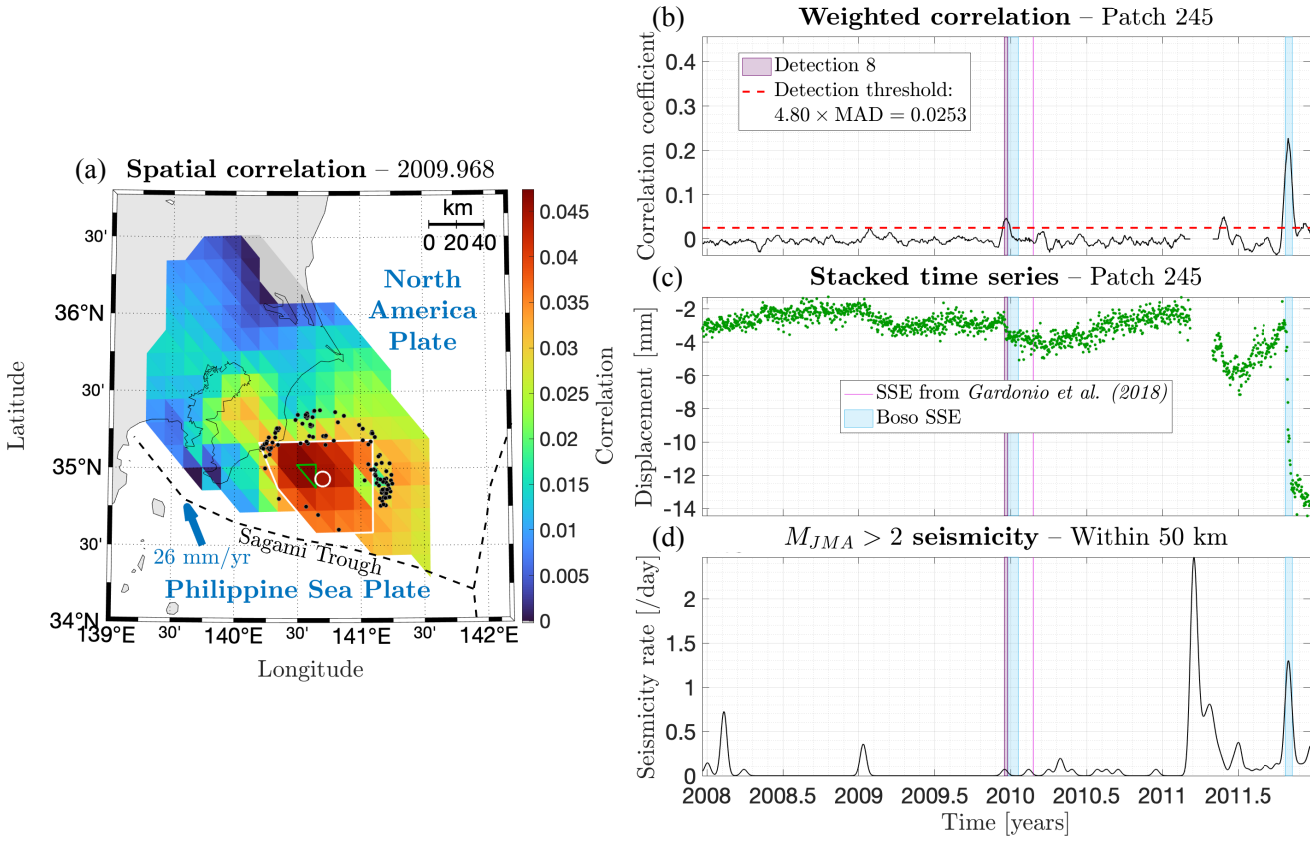

Figure S12. Same as Figure S4, but for event 8 detected on the PHS plate.

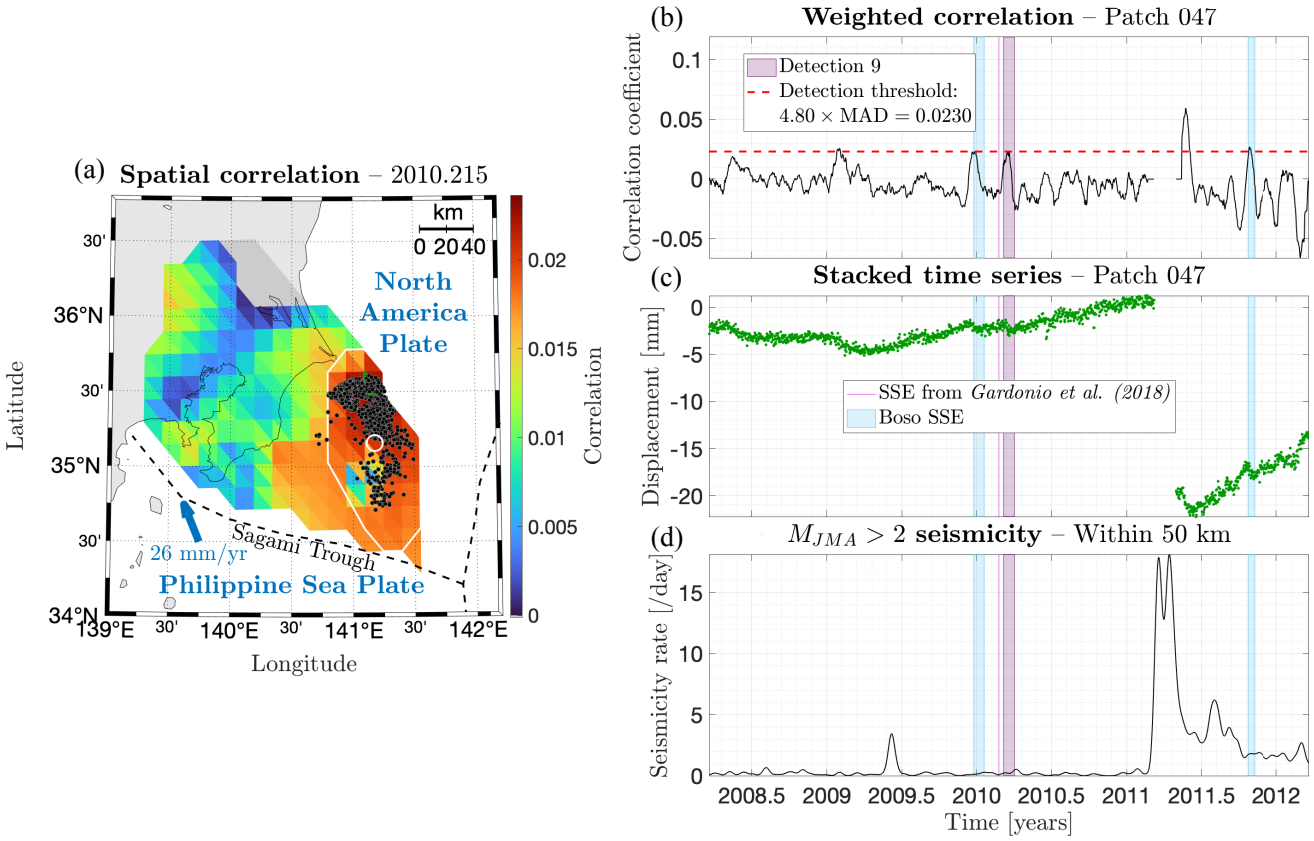

Figure S13. Same as Figure S4, but for event 9 detected on the PHS plate.

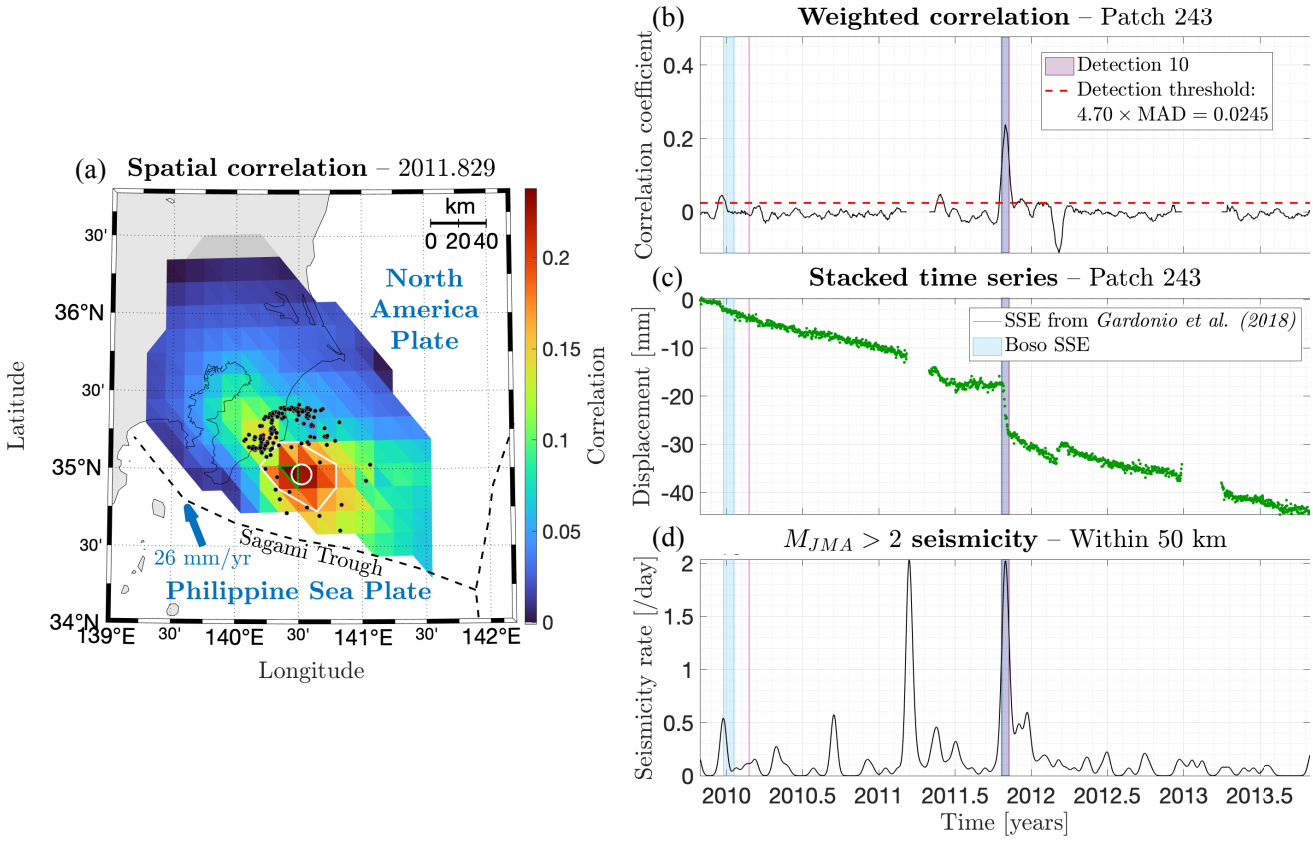

Figure S14. Same as Figure S4, but for event 10 detected on the PHS plate.

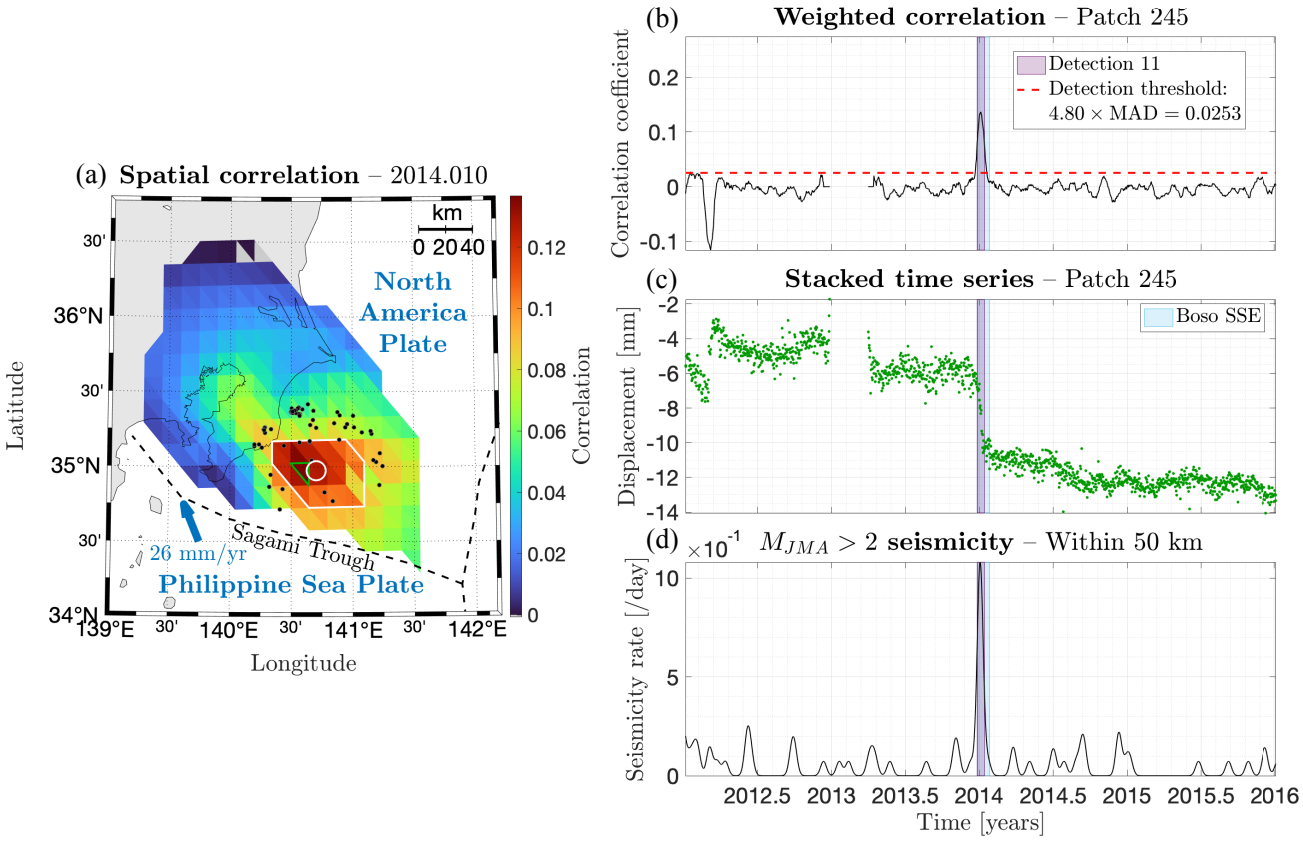

Figure S15. Same as Figure S4, but for event 11 detected on the PHS plate.

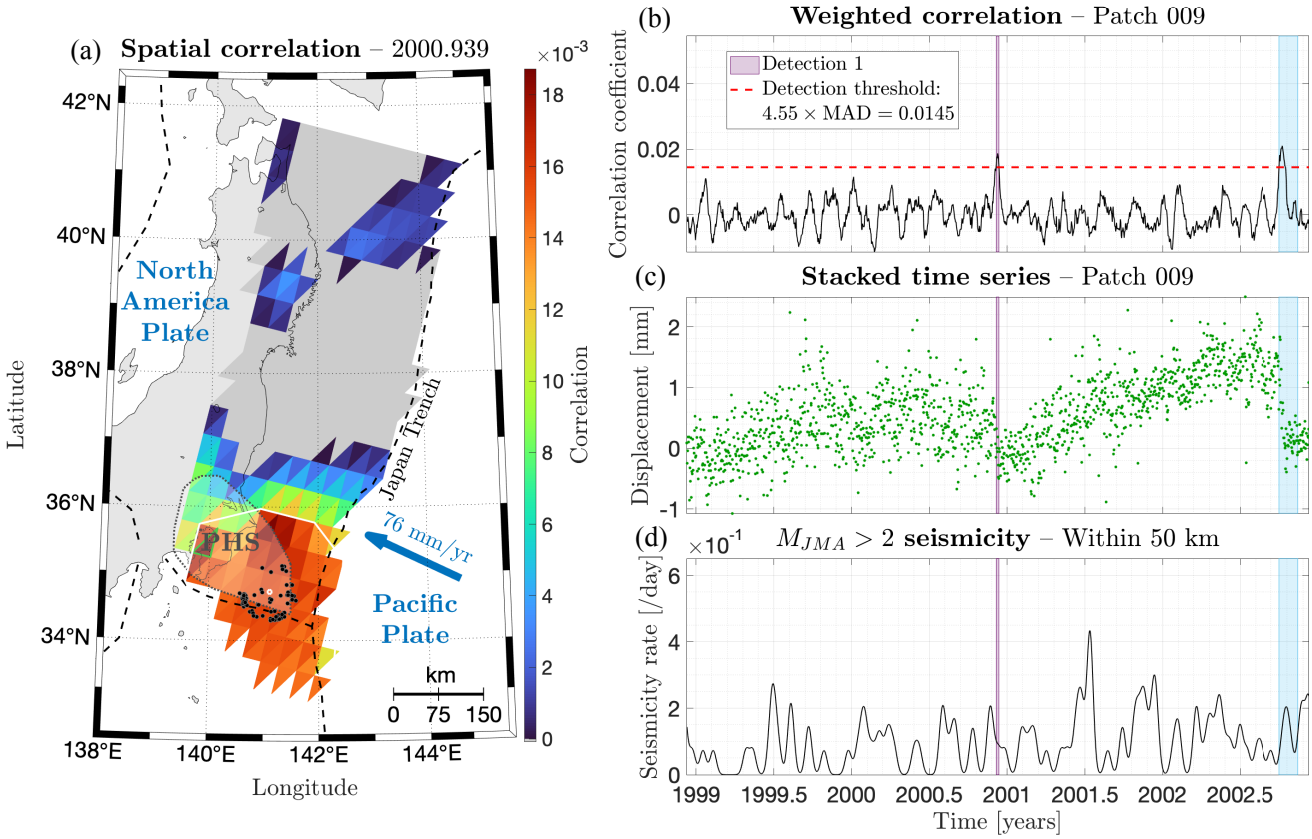

Figure S16. Same as Figure S4, but for event 1 detected on the PAC plate.

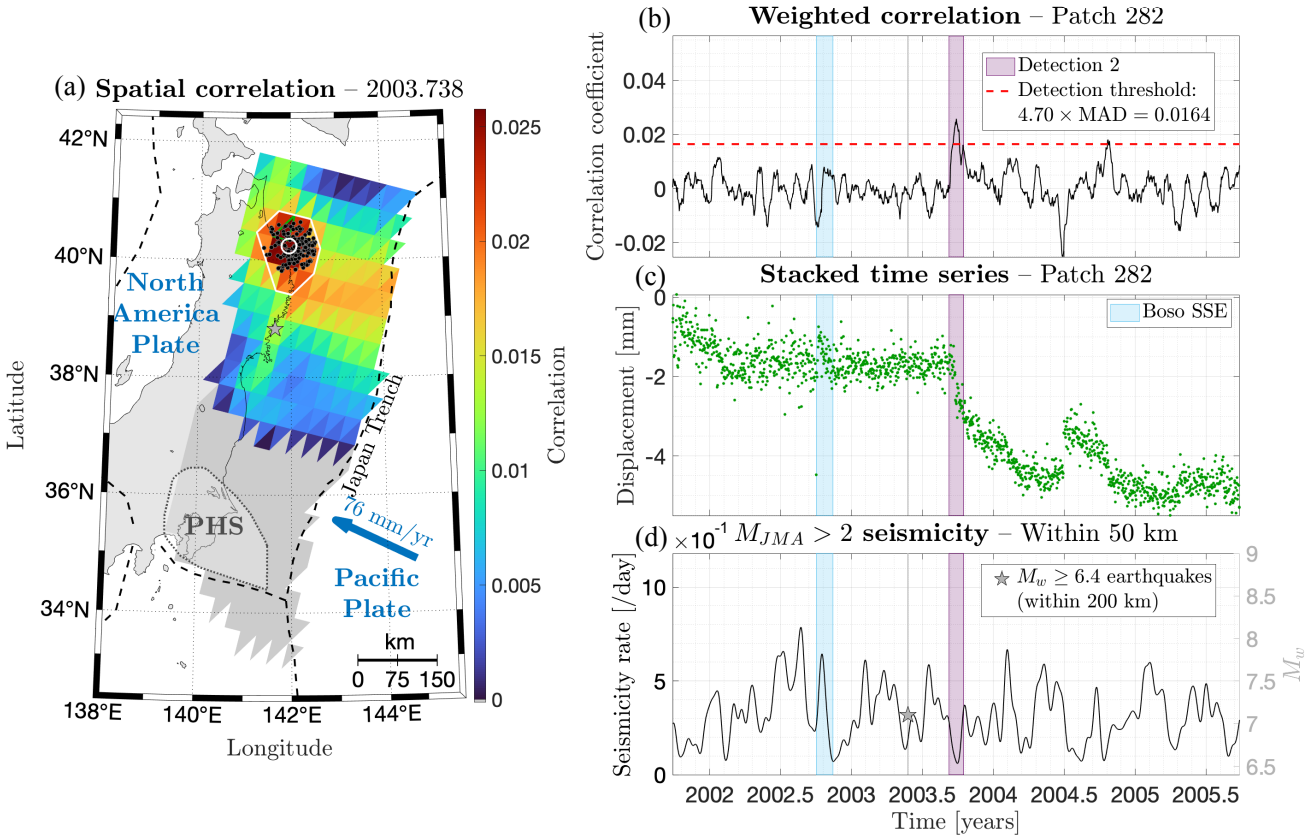

Figure S17. Same as Figure S4, but for event 2 detected on the PAC plate.

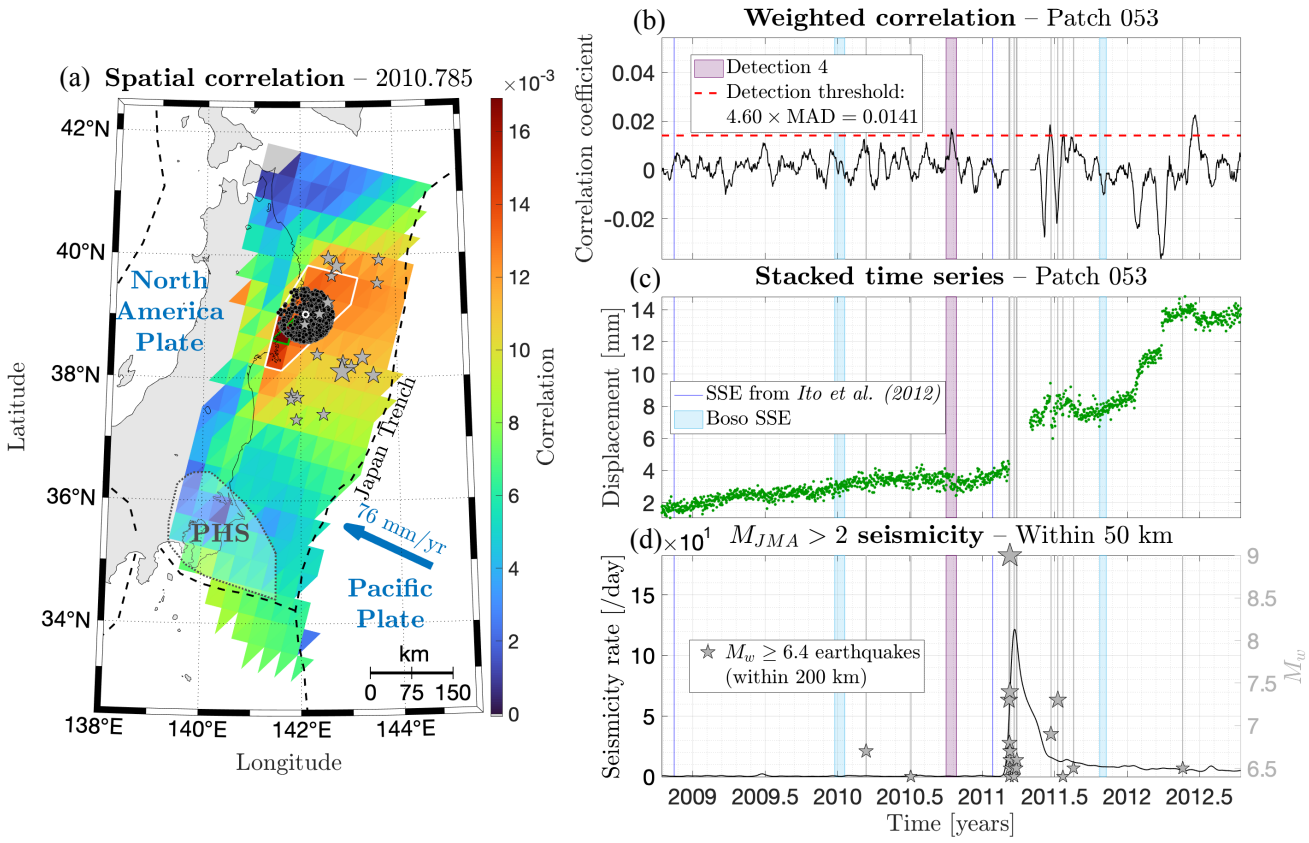

Figure S18. Same as Figure S4, but for event 4 detected on the PAC plate.

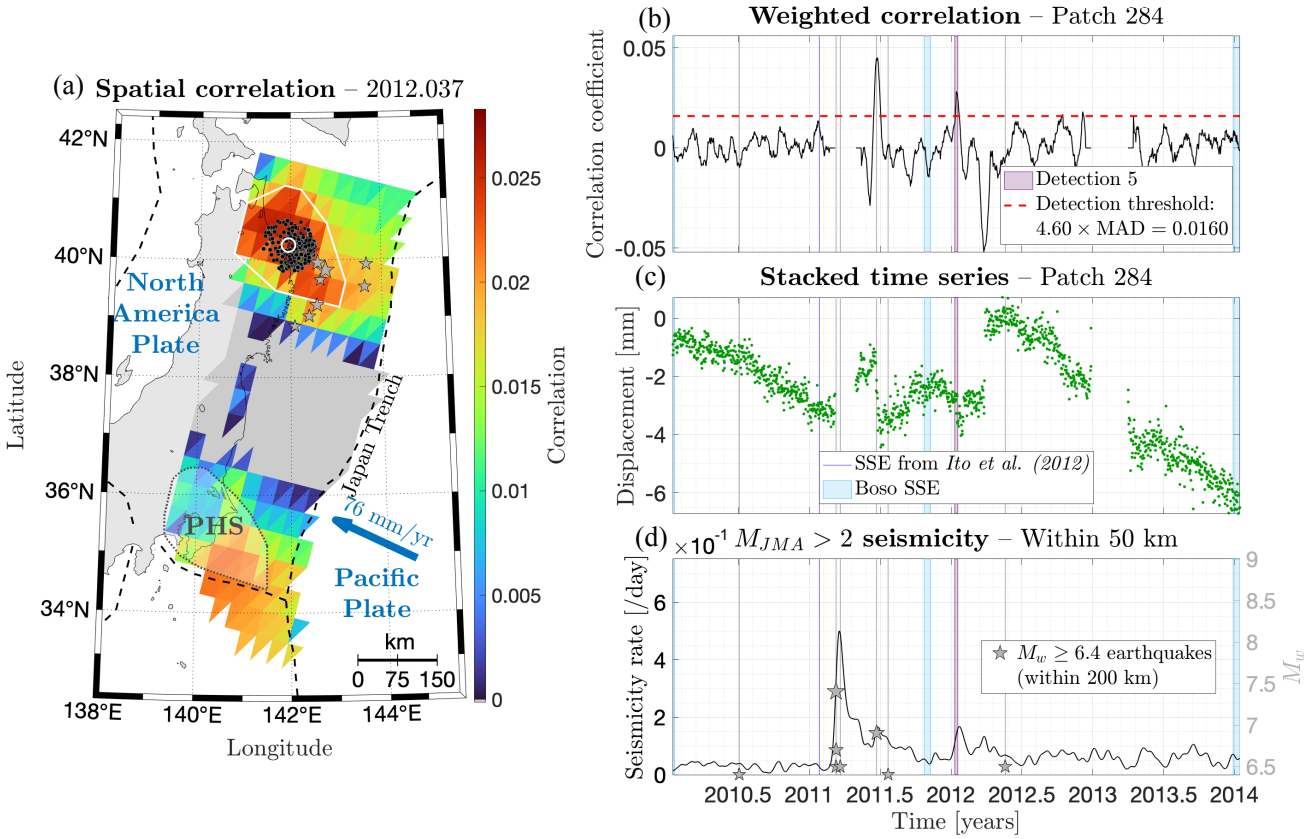

Figure S19. Same as Figure S4, but for event 5 detected on the PAC plate.

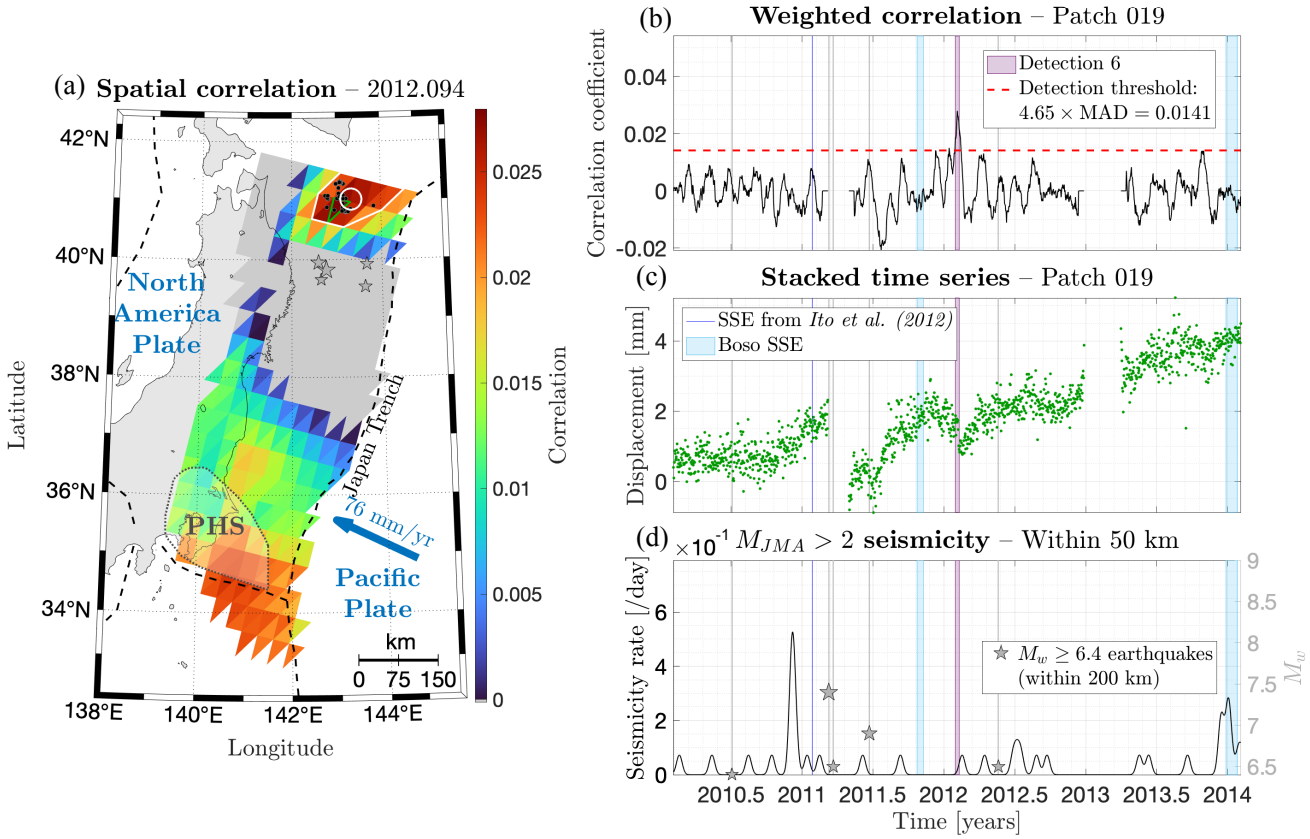

Figure S20. Same as Figure S4, but for event 6 detected on the PAC plate.

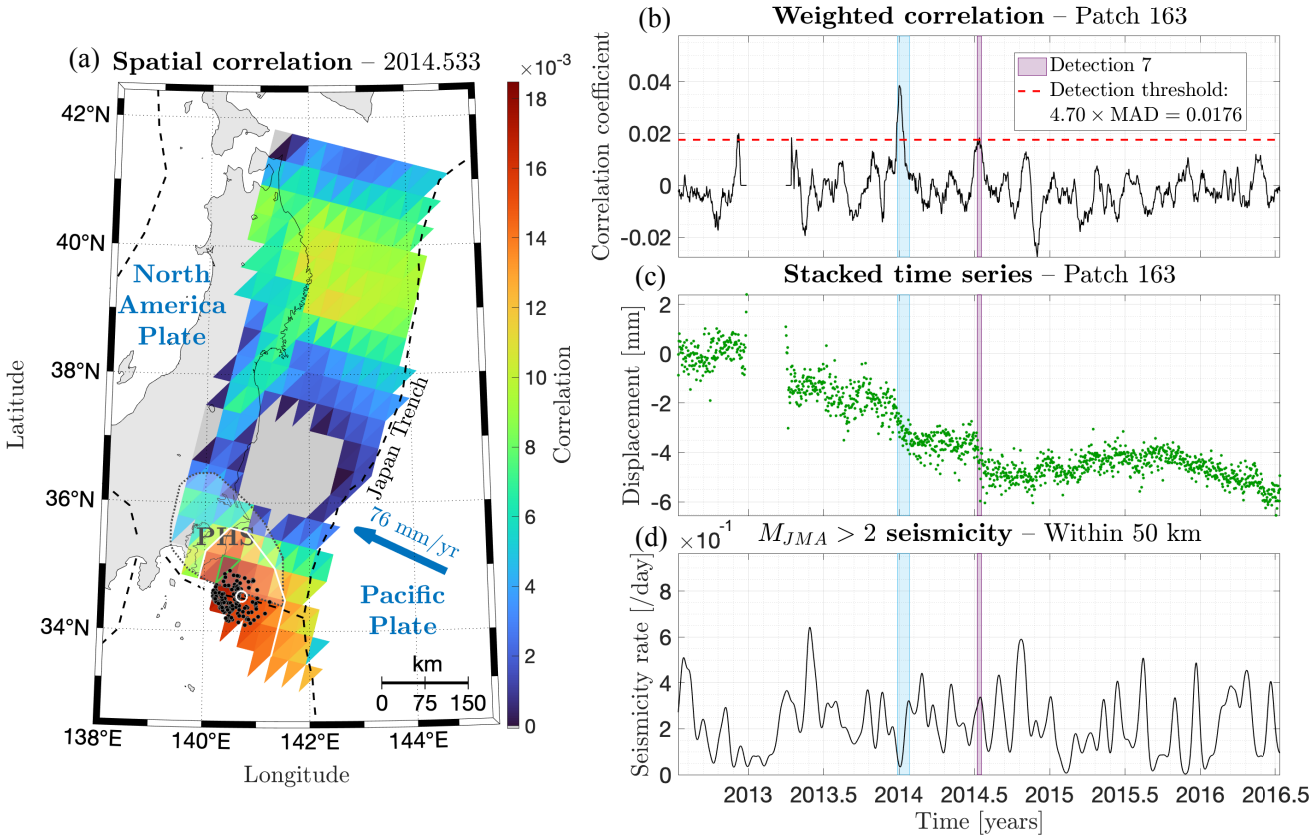

Figure S21. Same as Figure S4, but for event 7 detected on the PAC plate.

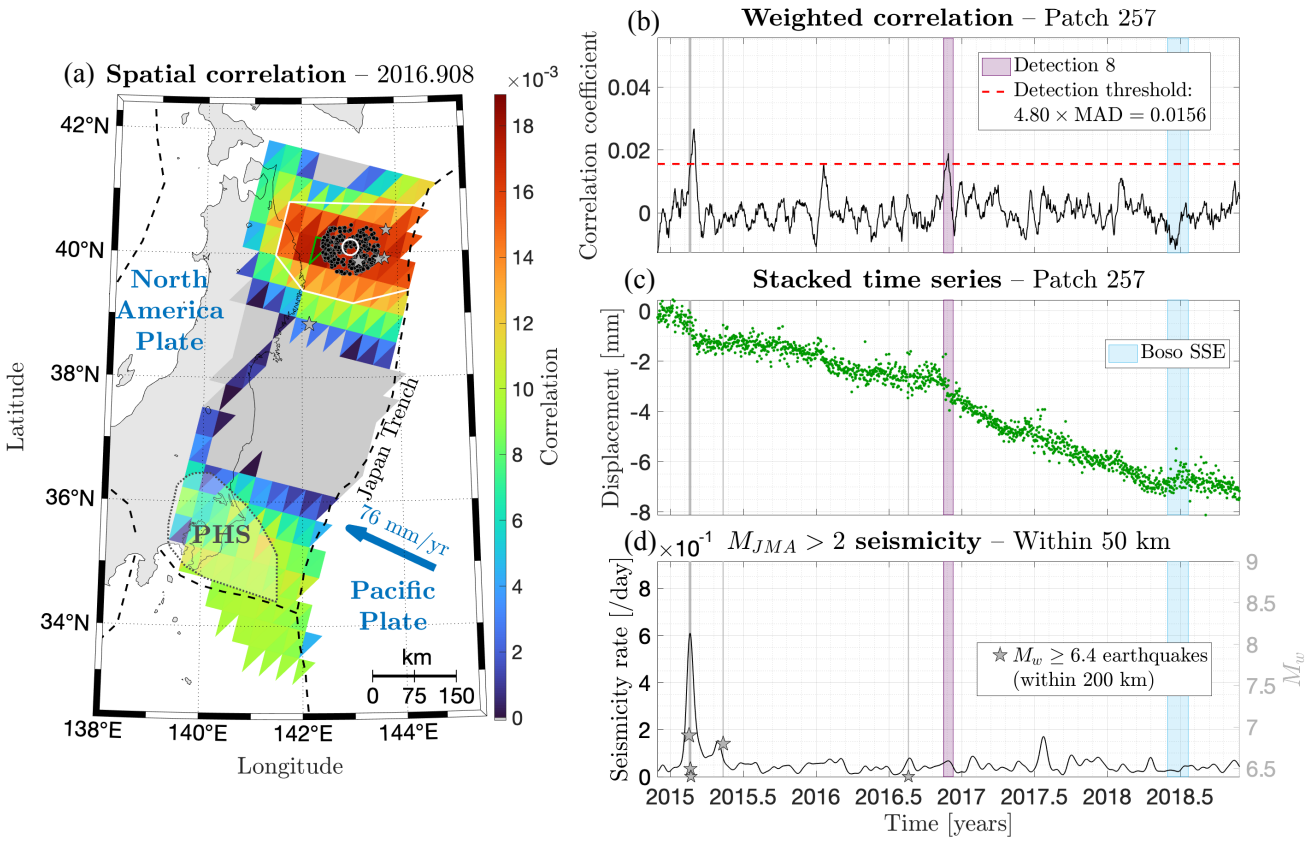

Figure S22. Same as Figure S4, but for event 8 detected on the PAC plate.

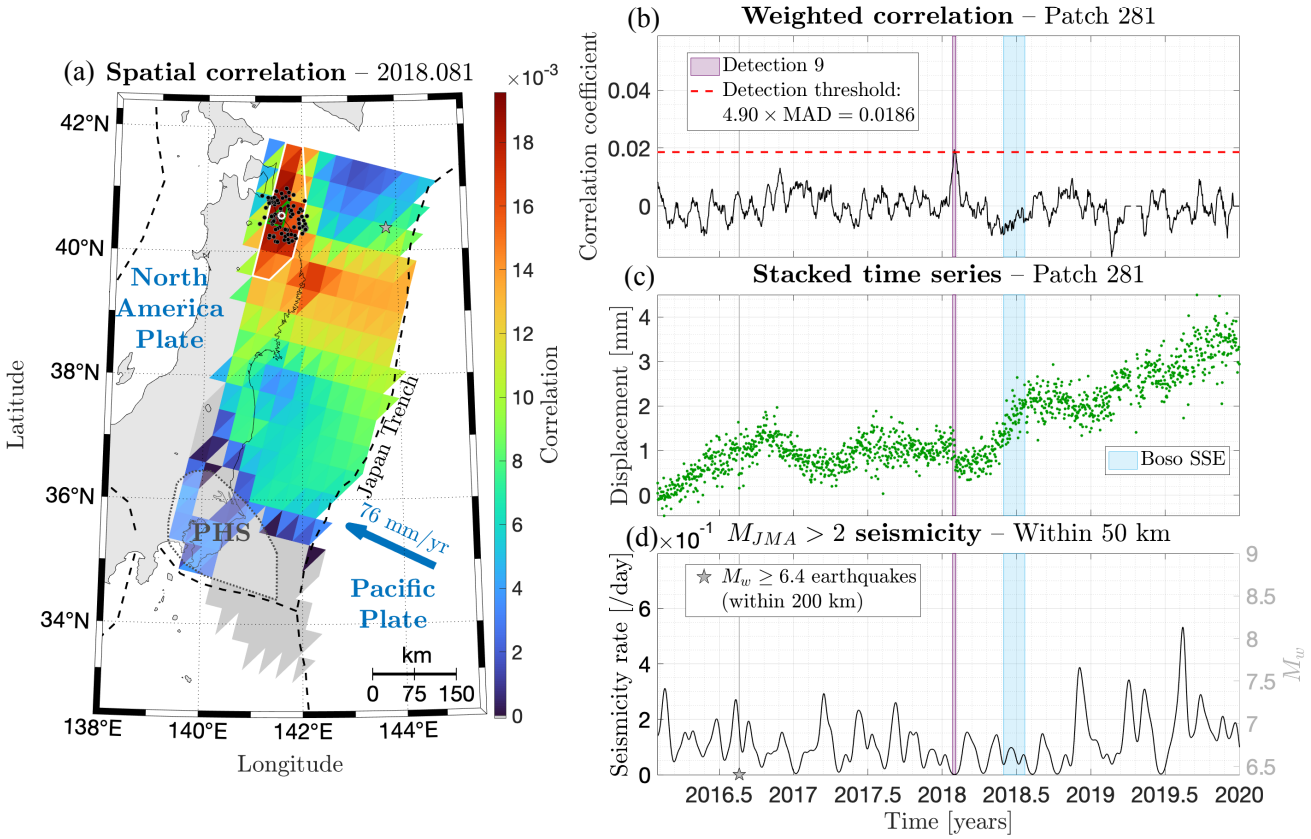

Figure S23. Same as Figure S4, but for event 9 detected on the PAC plate.

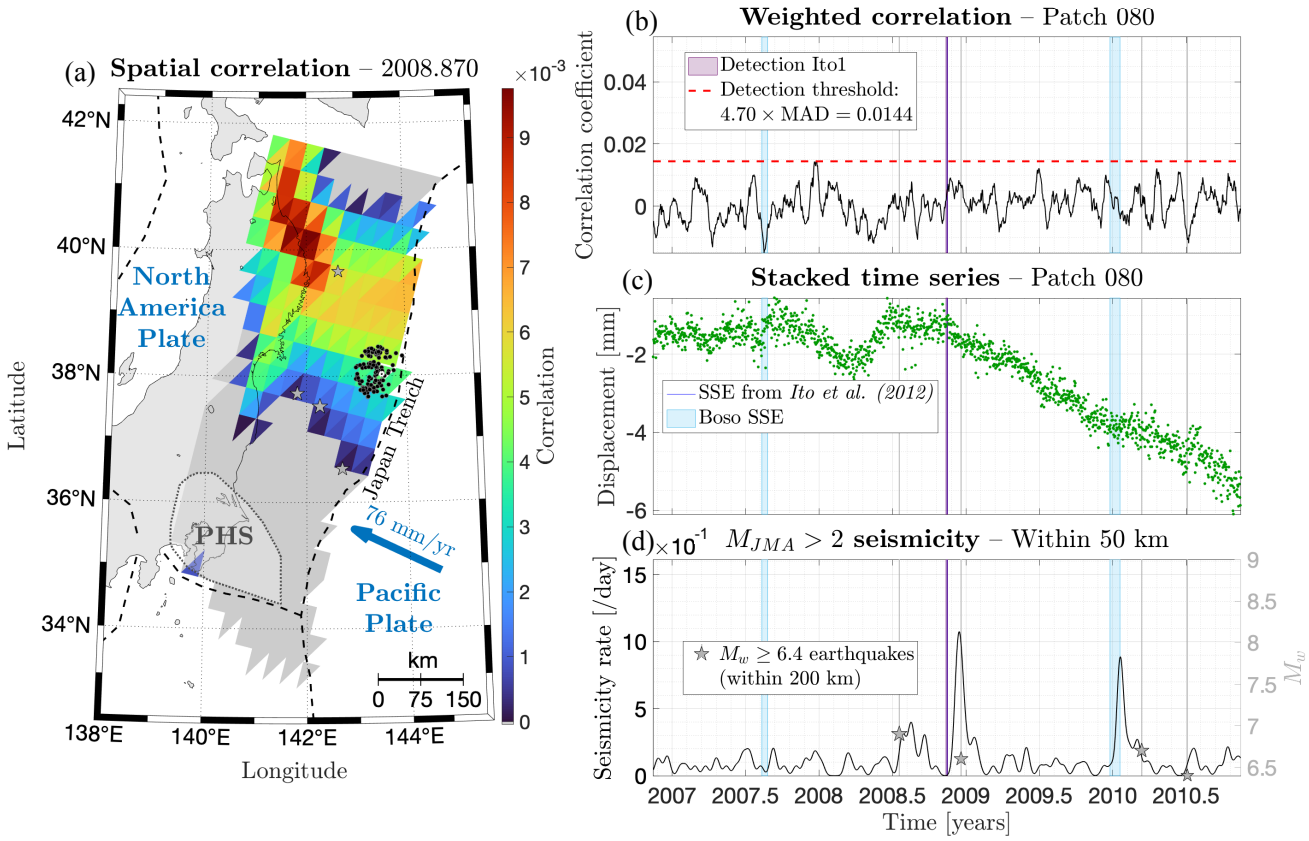

Figure S24. Correlation at the time of the 2008 SSE from Ito et al. (2012). (a) Amplitude of the correlation on the plate interface. The white circle highlights the location of Ito et al., (2012) SSEs. (b), (c) and (d) Same as Figure S4.

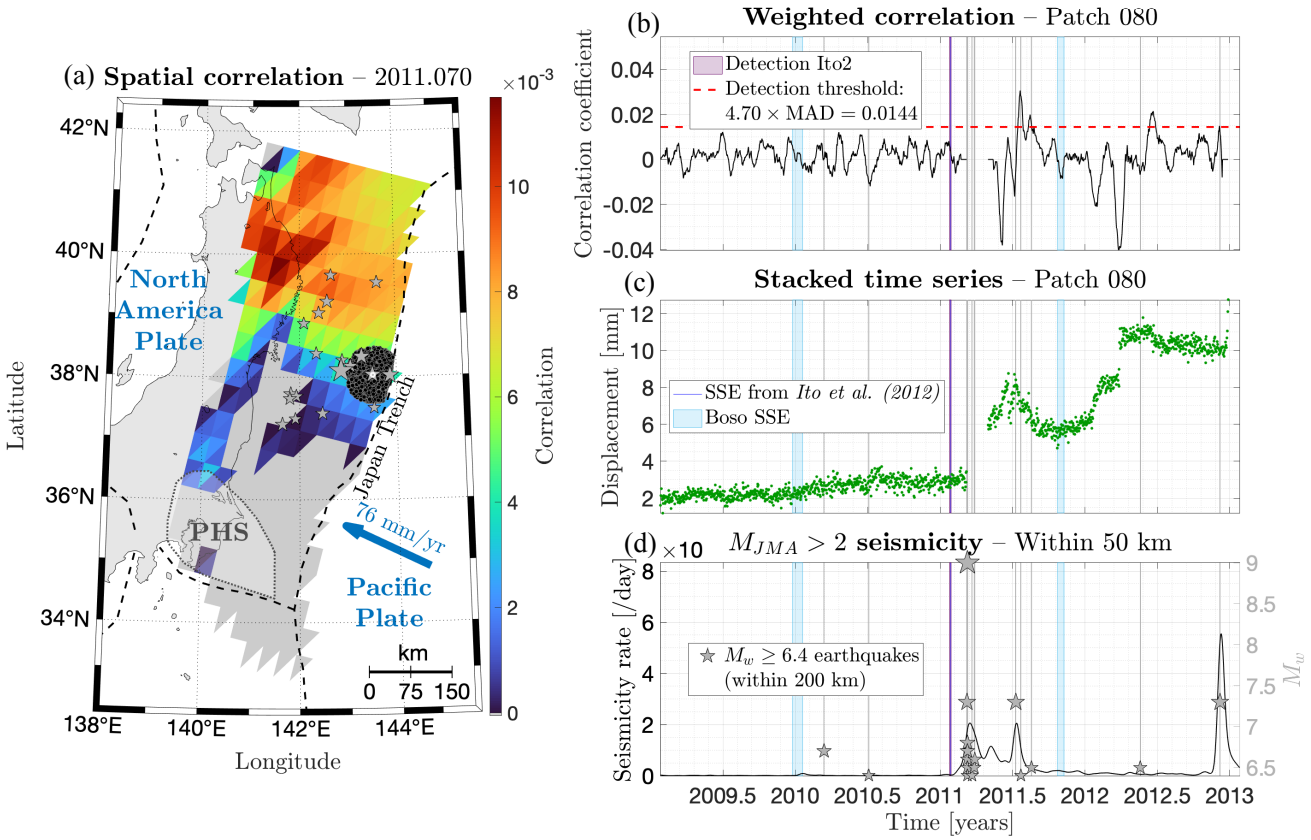

Figure S25. Same as Figure S23, but at the time of the 2011 SSE from Ito et al. (2012).